Supporting Information for

Pyrolysis-free synthesis of high-loading single-atomic Cu catalyst for efficient electrocatalytic CO_2-to-CH_4 conversion

Jiawei Li,[a, b †] Yawen Jiang,[c, †] Jiayi Li,[a] Xinyu Wang,[a, b] Hengjie Liu,[a] Ning Zhang,[a, b], Ran Long,[a]* and Yujie Xiong,[a, b]**

[a] National Synchrotron Radiation Laboratory, Hefei National Research Center for Physical Sciences at the Microscale, Key Laboratory of Precision and Intelligent Chemistry, School of Chemistry and Materials Science, Department of Environmental Science and Engineering, University of Science and Technology of China, Hefei, Anhui 230026, China

[b] Sustainable Energy and Environmental Materials Innovation Center, Suzhou Institute for Advanced Research, University of Science and Technology of China, Suzhou, Jiangsu 215123, China

[c] Deep Space Exploration Laboratory, Hefei, Anhui 230026, China

[†] These authors contributed equally to this work.

E-mail: zhangning18@ustc.edu.cn (N.Z.); longran@ustc.edu.cn (R.L.); yjxiong@ustc.edu.cn (Y.X.)

Supplementary experimental section

Chemicals.

Iridium chloride(III) hydrate was purchased from Macklin. Nafion (R) perfluorinated resin solution (5 wt. % in aliphatic alcohols and water) was purchased from Sigma-Aldrich. Sustainion XA-9 ionomer (5 wt%) was purchased from Dioxide Materials. All other chemicals used in the experiments are of analytical grade and purchased from Sinopharm Chemical Reagent Co., Ltd. Deionized water (18.25 MΩ·cm) was used in all experiments. All the chemicals were used as received without any further purification.

Sample characterizations.

Transmission electron microscopy (TEM) images, scanning transmission electron microscopy (STEM) images, high-resolution TEM (HRTEM) images and energy-dispersive X-ray spectroscopy (EDS) mapping profiles were collected on the Talos F200X and JEOL JEM-F200 transmission electron microscope. Aberration-corrected high-angle annular dark-field scanning transmission electron microscopy (HAADF-STEM) images were taken on a Themis Z instrument at 300 keV. Inductively coupled plasma-atomic emission spectrometry (ICP-AES) measurements were performed on the Optima 7300 DV spectrometer. The samples were added into 1mL aqua regia. After complete digestion of the samples, 9 mL of deionized water was added and the final solutions were used for the analysis. Powder X-ray diffraction (XRD) patterns were recorded using a a Philips X'Pert Pro Super X-ray diffractometer with Cu-Kα radiation (λ = 1.5418 Å). X-ray photoelectron spectra (XPS) were acquired on an ESCALAB250 X-ray photoelectron spectrometer, using non-monochromatic Al-Kα X-ray as the excitation source. All the XPS spectra were calibrated according to the C 1s peak at 284.8 eV. Fourier transform infrared (FTIR) spectroscopy was performed using a Thermo Nicolet 6700 spectrometer. Cu K-edge XAFS characterization was performed at the beamline BL14W1 of Shanghai Synchrotron Radiation Facility (SSRF, China). N and C K-edge XAFS characterizations were performed at the MCD Endstation (BL12B) of the National Synchrotron Radiation Laboratory (NSRL, China).

Preparation of gas diffusion electrode (GDE) used in flow cell.

8 mg of the FAP-Cu-x or FAP and 30 µL of Nafion solution (5wt%) or Sustainion XA-9 ionomer (5wt%) were added into 1.97 mL of isopropyl alcohol. The mixture was ultrasonically treated for at least 30 min to obtain a homogeneous catalyst ink. Then, 200 µL of catalyst ink was dropped onto a 1.5 cm × 1.5 cm gas diffusion layer (GDL, YLS-30T) and dried under a heating lamp. The catalyst loading was about 0.36 mg/cm^2.

Preparation of GDE used in MEA electrolyzer.

10 mg of the FAP-Cu-0.6 and 100 µL of Sustainion XA-9 ionomer (5wt%) were added into 1.9 mL of isopropyl alcohol. The mixture was ultrasonically treated for at least 30 min to obtain a homogeneous catalyst ink. Then, 625 µL of catalyst ink was dropped onto a 2.5 cm × 2.5 cm GDL (YLS-30T) and dried under a heating lamp. The catalyst side of the GDE was immersed into 1-M KOH for at least 4 h to change the Sustainion XA-9 ionomer from Cl^- mode to OH^- mode.

Preparation of IrO_x/Ti electrode.

A titanium foam with the size of 2.5 cm × 2.5 cm was etched in boiling 0.5-M oxalic acid solution for 60 min. The etched titanium foam was rinsed with deionized water and dried, and then immersed in 50 mL of isopropyl alcohol solution containing 30-mg $IrCl_3 \cdot xH_2O$ and 10% concentrated hydrochloric acid by volume. The titanium foam was taken out and dried with a heating lamp, and then calcined in the air for 10 min at 500 °C in a tube furnace. The soaking and calcination process was repeated until the catalyst load reaching 1 mg/cm^2. The obtained electrode was denoted as IrO_x/Ti.

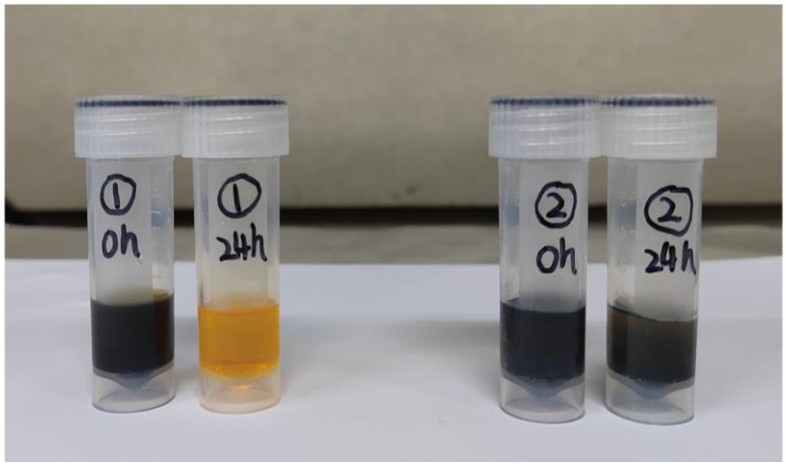

Fig. S1 Photograph of the FAP-Cu-0.6 (labelled as 1) and carbon black (labelled as 2) before and after immersed in aqua regia for 24 h.

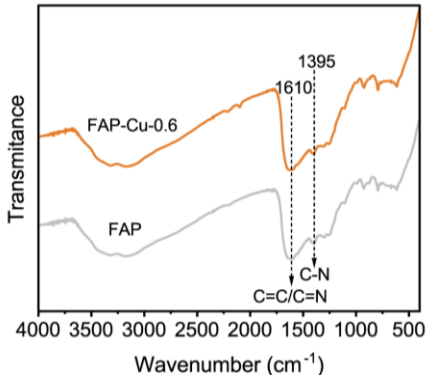

Fig. S2 FT-IR spectroscopy of the FAP-Cu-0.6 and FAP samples.

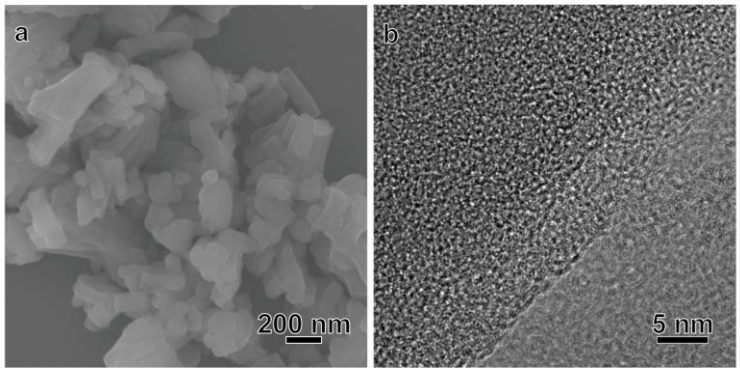

Fig. S3 SEM image (a) and HRTEM image (b) of the FAP-Cu-0.6 sample.

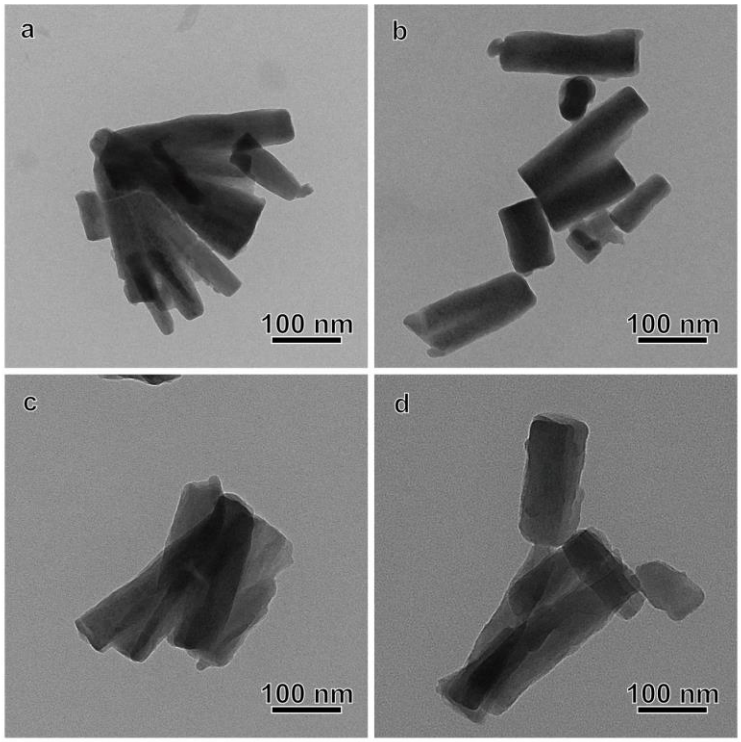

Fig. S4 TEM images of FAP (a), FAP-Cu-0.3 (b), FAP-Cu-1.2 (c) and FAP-Cu-1.8 (d) samples.

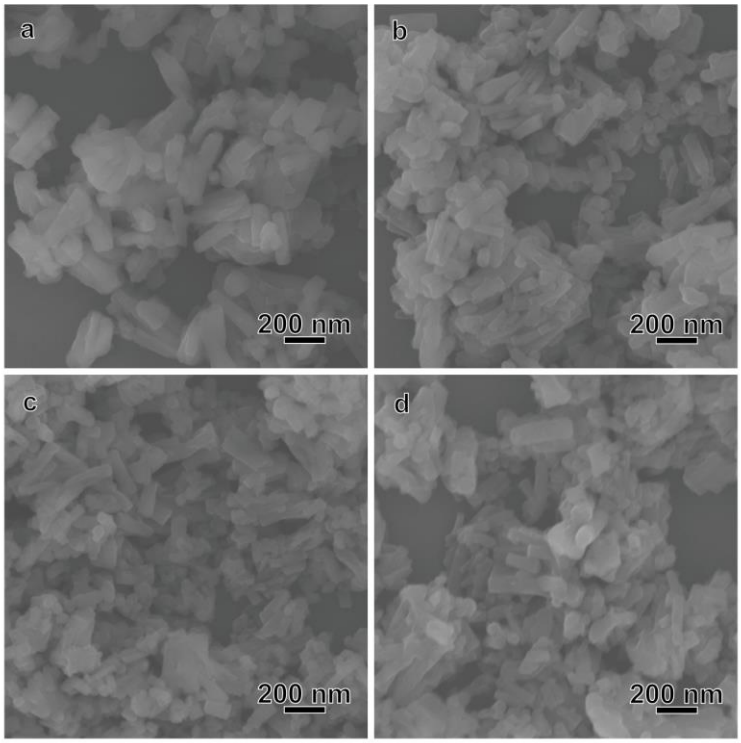

Fig. S5 SEM images of FAP (a), FAP-Cu-0.3 (b), FAP-Cu-1.2 (c) and FAP-Cu-1.8 (d) samples.

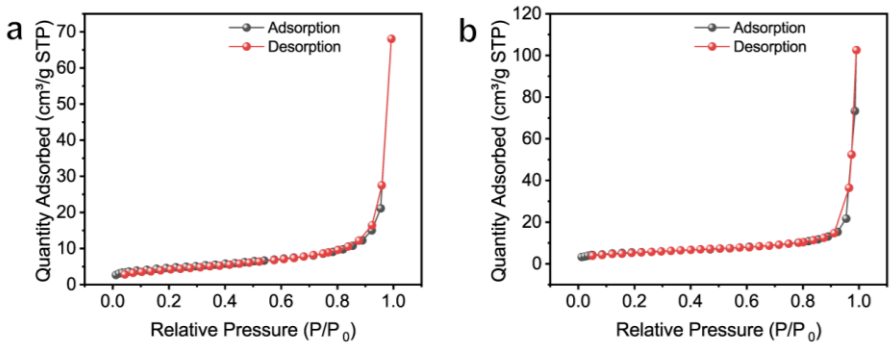

Fig. S6 N_2 sorption isotherms of FAP (a) and FAP-Cu-0.6 (b) at 77 K.

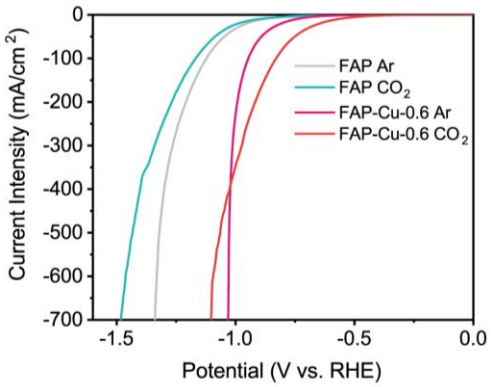

Fig. S7 LSV curves of CO_2RR in a flow cell supplied with CO_2 and Ar over FAP and FAP-Cu-0.6 catalysts.

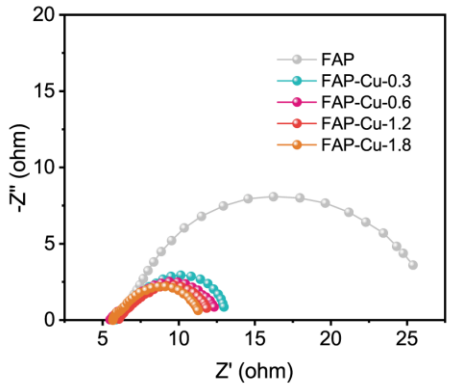

Fig. S8 The Nyquist plots of the FAP-Cu-x samples.

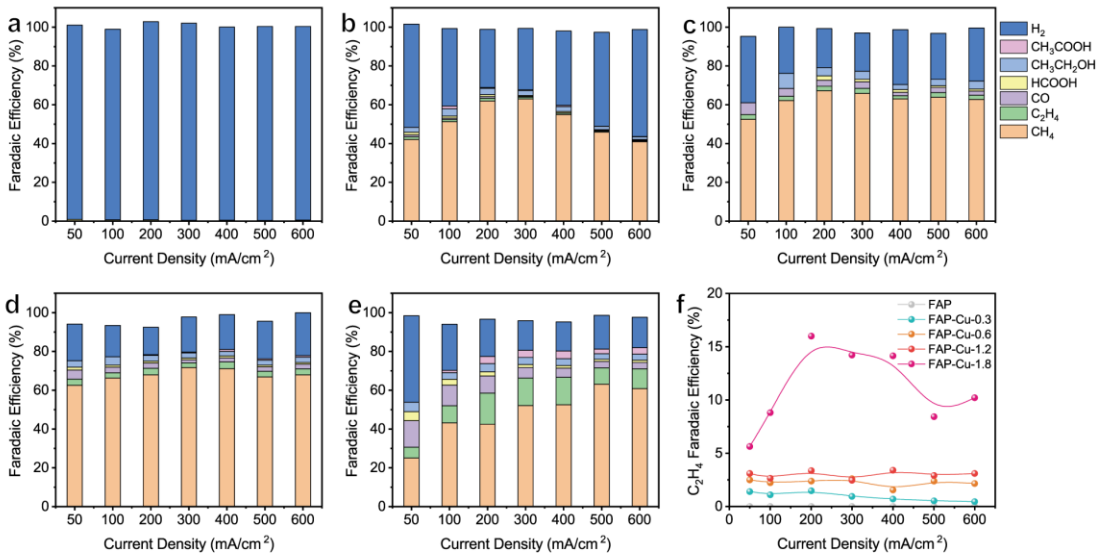

Fig. S9 The FE distribution of all products for FAP (a), FAP-Cu-0.3 (b), FAP-Cu-0.6 (c), FAP-Cu-1.2 (d) and FAP-Cu-1.8 (e) catalysts, respectively. (f) The determined C_2H_4 FEs for various catalysts.

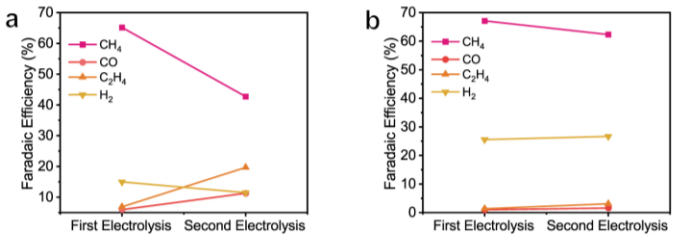

Fig. S10 The FEs of gas products of two continuously chronoamperometric electrolysis at 300 mA/cm^2 for FAP-Cu-1.2 (a) and FAP-Cu-0.6 (b). Each electrolysis process was performed for 600 s.

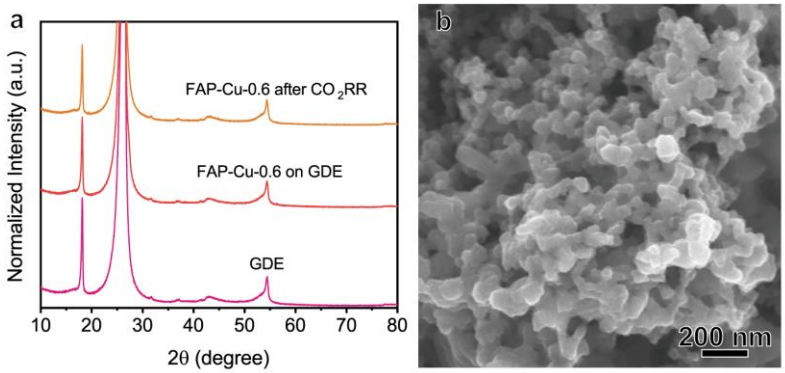

Fig. S11 (a) The XRD patterns of GDE, FAP-Cu-0.6 before and after CO_2RR. (b) The SEM image of FAP-Cu-0.6 after CO_2RR.

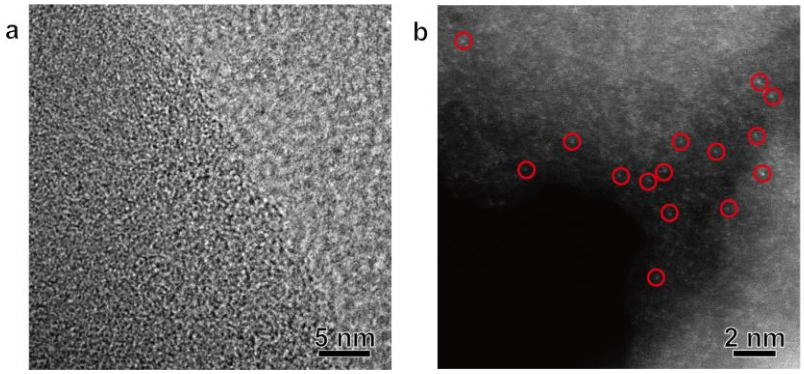

Fig. S12 HRTEM image (a) and aberration-corrected HAADF-STEM image (b) of the FAP-Cu-0.6 catalyst after CO_2RR.

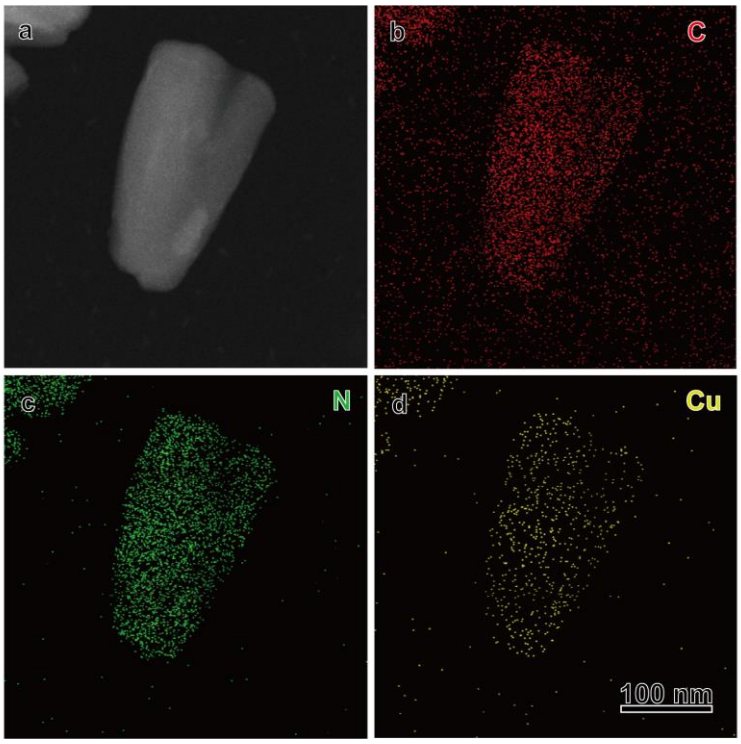

Fig. S13 HAADF−STEM image (a) and corresponding EDS elemental mapping images of C (b), N (c), and Cu (d) in the FAP-Cu-0.6 catalyst after electrolysis.

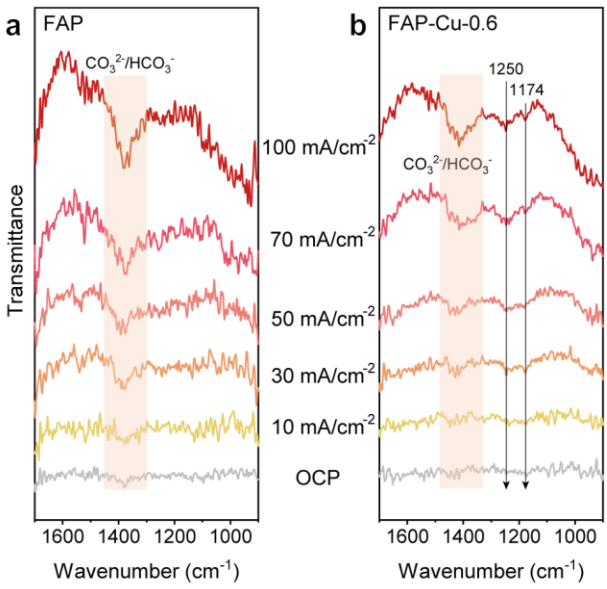

Fig. S14 *In-situ* SR-FTIR spectroscopy for FAP (a) and FAP-Cu-0.6 (b).

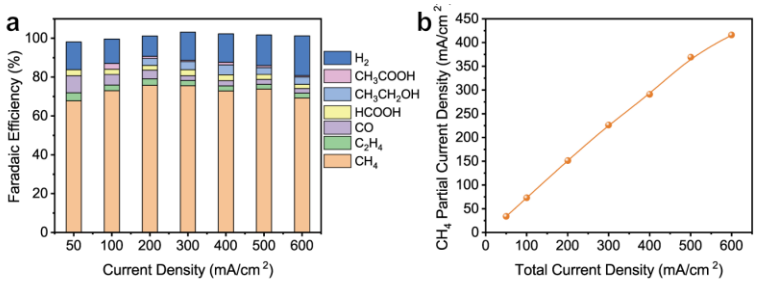

Fig. S15 (a) The FE values of all products for FAP-Cu-0.6 catalyst using Sustainion XA-9 ionomer as binder. (b) The calculated CH_4 partial current densities over FAP-Cu-0.6 catalyst using Sustainion XA-9 ionomer as binder.

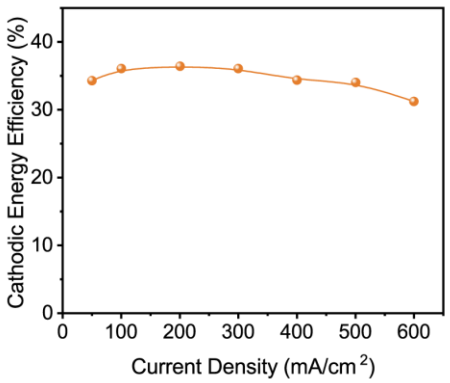

Fig. S16 The CEE values of CH4 for FAP-Cu-0.6 using Sustainion XA-9 ionomer at different applied current densities.

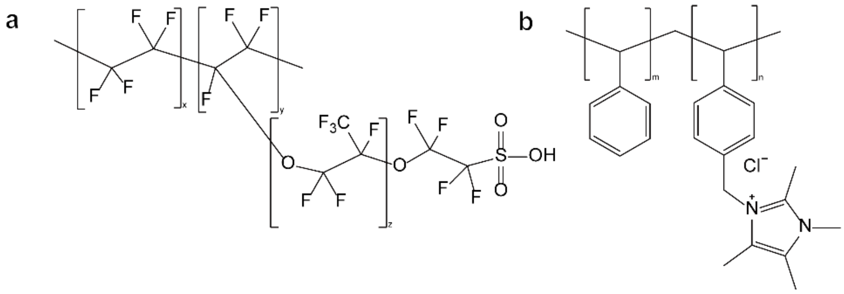

Fig. S17 The chemical structure of Nafion (a) and Sustainion XA-9 ionomer (b).

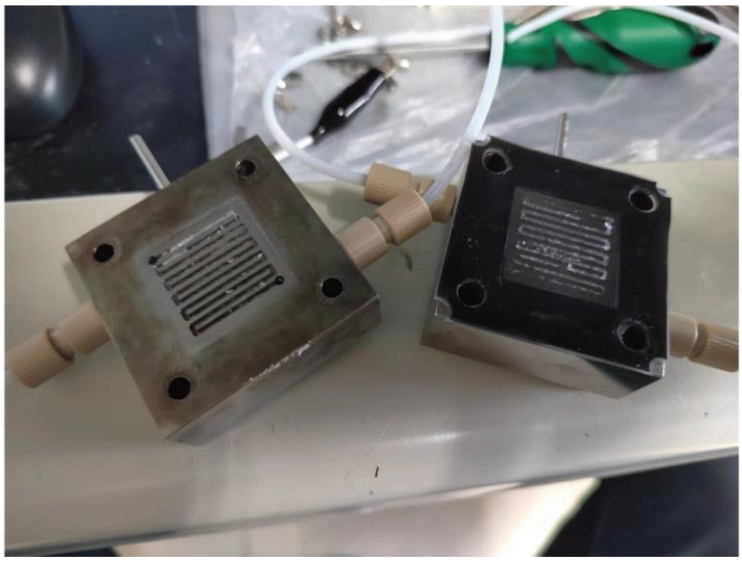

Fig. S18 Photograph of the GDE and the channel of the cathode after stability test.

Table S1. The exact Cu contents in the series samples.

Sample	Cu content (wt%)
FAP-Cu-0.3	3.60
FAP-Cu-0.6	5.87
FAP-Cu-1.2	10.59
FAP-Cu-1.8	13.99

Table S2. Fitting Results of Cu K-Edge EXAFS Data[a].

Sample	Scattering Path	CN	R(Å)	σ^2 (Å)
FAP-Cu-0.6	Cu-N	4.39 ± 0.36	1.93 ± 0.07	0.00774

[a]CN, the coordination numbers; R, the bonding distance; σ^2, the Debye-Waller factor; S_0^2 for Cu-N was set as 0.8.

Table S3. Comparison of CH_4 FEs for the recently reported Cu-based electrocatalysts.

Catalyst	Reactor	Electrolyte	J_{CH4} (mA/cm^2)	CH_4 FE	Ref.
FAP-Cu-0.6	**Flow cell**	**1 M KOH**	**415.8**	**69.3%**	**This work**
FAP-Cu-0.6	**Flow cell**	**1 M KOH**	**151.4**	**75.7%**	**This work**
Cu-Ce-O_x	Flow cell	1 M KOH	135.6	67.8%	1
7% Au-Cu	Flow cell	1 M $KHCO_3$	112	56%	2
NNU-33(H)	Flow cell	1 M KOH	321.9	82%	3
Cu-DBC	Flow cell	1 M KOH	162.4	80%	4
Cu-TDPP-NS	Flow cell	0.5 M PBS	128.1	70%	5
La_2CuO_4	Flow cell	1 M KOH	117	56.3%	6
Cu/Al_2O_3	Flow cell	1 M KOH	94.8	62%	7
Sputter Cu on PTFE	Flow cell	1 M $KHCO_3$	108	48%	8
Carbon coated on Cu/Cu_2O	Flow cell	1 M KOH	366.5	73.3%	9
Carbon coated on Cu/Cu_2O	H-cell	0.1 M $KHCO_3$	39	81%	9
Cu cluster/DRC	H-cell	0.1 M $KHCO_3$	18	81.7%	10
$Ag@Cu_2O$	Flow cell	1 M KOH	178	74%	11
$20\%Cu/MgSiO_3$	Flow cell	1 M KOH	432.3	72.05%	12
CuFe-SA	Flow cell	1 M $KHCO_3$	128	64%	13
CeO_2 cluster-7% Cu	Flow cell	1 M KOH	268.5	67.1%	14
Cu PTI	Flow cell	1 M KOH	348	68%	15

References

1. X. Zhou, J. Shan, L. Chen, B. Y. Xia, T. Ling, J. Duan, Y. Jiao, Y. Zheng and S.-Z. Qiao, *J. Am. Chem. Soc.*, 2022, **144**, 2079-2084.
2. X. Wang, P. Ou, J. Wicks, Y. Xie, Y. Wang, J. Li, J. Tam, D. Ren, J. Y. Howe, Z. Wang, A. Ozden, Y. Z. Finfrock, Y. Xu, Y. Li, A. S. Rasouli, K. Bertens, A. H. Ip, M. Graetzel, D. Sinton and E. H. Sargent, *Nat. Commun.*, 2021, **12**, 3387.
3. L. Zhang, X.-X. Li, Z.-L. Lang, Y. Liu, J. Liu, L. Yuan, W.-Y. Lu, Y.-S. Xia, L.-Z. Dong, D.-Q. Yuan and Y.-Q. Lan, *J. Am. Chem. Soc.*, 2021, **143**, 3808-3816.
4. Y. Zhang, L.-Z. Dong, S. Li, X. Huang, J.-N. Chang, J.-H. Wang, J. Zhou, S.-L. Li and Y.-Q. Lan, *Nat. Commun.*, 2021, **12**, 6390.
5. Y. R. Wang, M. Liu, G. K. Gao, Y. L. Yang, R. X. Yang, H. M. Ding, Y. Chen, S. L. Li and Y. Q. Lan, *Angew. Chem. Int. Ed.*, 2021, **60**, 21952-21958.
6. S. Chen, Y. Su, P. Deng, R. Qi, J. Zhu, J. Chen, Z. Wang, L. Zhou, X. Guo and B. Y. Xia, *ACS Catal.*, 2020, **10**, 4640-4646.
7. S. Chen, B. Wang, J. Zhu, L. Wang, H. Ou, Z. Zhang, X. Liang, L. Zheng, L. Zhou, Y.-Q. Su, D. Wang and Y. Li, *Nano Lett.*, 2021, **21**, 7325-7331.
8. X. Wang, A. Xu, F. Li, S.-F. Hung, D.-H. Nam, C. M. Gabardo, Z. Wang, Y. Xu, A. Ozden, A. S. Rasouli, A. H. Ip, D. Sinton and E. H. Sargent, *J. Am. Chem. Soc.*, 2020, **142**, 3525-3531.
9. X. Y. Zhang, W. J. Li, X. F. Wu, Y. W. Liu, J. Chen, M. Zhu, H. Y. Yuan, S. Dai, H. F. Wang, Z. Jiang, P. F. Liu and H. G. Yang, *Energy Environ. Sci.*, 2022, **15**, 234-243.
10. Q. Hu, Z. Han, X. Wang, G. Li, Z. Wang, X. Huang, H. Yang, X. Ren, Q. Zhang, J. Liu and C. He, *Angew. Chem. Int. Ed.*, 2020, **59**, 19054-19059.
11. L. Xiong, X. Zhang, L. Chen, Z. Deng, S. Han, Y. Chen, J. Zhong, H. Sun, Y. Lian, B. Yang, X. Yuan, H. Yu, Y. Liu, X. Yang, J. Guo, M. H. Rümmeli, Y. Jiao and Y. Peng, *Adv. Mater.*, 2021, **33**, 2101741.
12. Y. Zhong, J. Low, Q. Zhu, Y. Jiang, X. Yu, X. Wang, F. Zhang, W. Shang, R. Long, Y. Yao, W. Yao, J. Jiang, Y. Luo, W. Wang, J. Yang, Z. Zou and Y. Xiong, *Nat. Sci. Rev.*, 2023, **10**, nwac200.
13. S.-F. Hung, A. Xu, X. Wang, F. Li, S.-H. Hsu, Y. Li, J. Wicks, E. G. Cervantes, A. S. Rasouli, Y. C. Li, M. Luo, D.-H. Nam, N. Wang, T. Peng, Y. Yan, G. Lee and E. H. Sargent, *Nat. Commun.*, 2022, **13**, 819.
14. Y. Jiang, K. Mao, J. Li, D. Duan, J. Li, X. Wang, Y. Zhong, C. Zhang, H. Liu, W. Gong, R. Long and Y. Xiong, *ACS Nano*, 2023, **17**, 2620-2628.
15. S. Roy, Z. Li, Z. Chen, A. C. Mata, P. Kumar, S. C. Sarma, I. F. Teixeira, I. F. Silva, G. Gao, N. V. Tarakina, M. G. Kibria, C. V. Singh, J. Wu and P. M. Ajayan, *Adv. Mater.*, 2023, DOI: 10.1002/adma.202300713.